

POLSAR SPECKLE FILTERING AND SEGMENTATION BASED ON BINARY PARTITION TREE REPRESENTATION

Alberto Alonso-González, Carlos López-Martínez, and Philippe Salembier

Universitat Politècnica de Catalunya (UPC), Signal Theory and Communications Dept. (TSC), Jordi Girona 1-3, 08034, Barcelona, Spain. Email: alberto.alonso@tsc.upc.edu

ABSTRACT

A region-based and multi-scale image representation is proposed in this work, the Binary Partition Tree (BPT), for different polarimetric SAR image processing applications. This structure contains a lot of information about the image structure at different detail levels. The BPT construction process and its exploitation for PolSAR data filtering and segmentation is analyzed in this work. Results with real and simulated data are presented to illustrate the capability of the BPT based filtering to maintain spatial resolution and small details of the image while, at the same time, strong filtering is performed over large homogeneous regions.

Key words: SAR, PolSAR, speckle filtering, segmentation, Binary Partition Tree.

1. INTRODUCTION

Synthetic Aperture Radar (SAR) is a technique that coherently combines the echoes received by a moving radar to form a high resolution image. In the last decade, multidimensional SAR data, specially polarimetric SAR data (PolSAR), have demonstrated its importance for characterization and classification of the earth surface. Some geophysical and biophysical information can be extracted by inversion of the polarimetric data.

However, SAR data are contaminated by speckle noise, produced by the coherent processing of received echoes. The speckle term can be reduced by estimation over homogeneous regions. However, SAR data are vastly non-homogeneous, as they reflect the structure of the scene. Some state-of-the-art techniques try to adapt to this non-stationarity, either with predefined directional windows [LGdG99] or defining an adaptive neighborhood for each pixel [VTLB06].

In this work we propose a Binary Partition Tree (BPT) [SG00] representation of the image to extract its spatial information in order to segment the data into homogeneous regions, where the polarimetric information can

be estimated precisely. The BPT is a fully region-based and multi-scale PolSAR data representation. Additionally this representation can be exploited for many different PolSAR processing applications. The BPT was introduced for PolSAR data processing in [AGLMS10]. In this paper, we introduce some new similarity criteria, and we do a more extensive evaluation with more complex and realistic synthetic data. Furthermore, we present results of coastline segmentation as a new application based on the BPT.

2. BINARY PARTITION TREE

The Binary Partition Tree (BPT) was introduced in [SG00] as a region-based and multi-scale image representation. It contains information of the image structure at different details levels within a tree. In this hierarchical structure each node represents a connected region of the image. The tree leaves represent single pixels and all the other nodes represent the region composed by merging its two son nodes. Finally, the root node represents the whole image. Thus, the tree edges describe the inclusion relationship between nodes. Between the leaf and the root there are a wide number of nodes representing regions of the image with different detail level. This multi-scale representation contains a lot of useful information about the image structure that can be exploited for different applications.

To construct the BPT representation from an image, an iterative algorithm is employed in a bottom-up approach [SG00]. In the initial state, every pixel of the image becomes a one-pixel region. At every step, the two most similar regions are merged and this process is repeated until the root of the tree, containing the whole image, is generated. In order to apply this algorithm, two important concepts have to be defined [AGLMS10]:

1. A region model: traditionally, under the complex Gaussian PolSAR model, the estimated covariance matrix \mathbf{Z} is employed to measure the region polari-

metric information

$$\mathbf{Z} = \langle \mathbf{k}\mathbf{k}^H \rangle_n = \frac{1}{n} \sum_{i=1}^n \mathbf{k}_i \mathbf{k}_i^H \quad (1)$$

where \mathbf{k}_i represents the scattering vector of the i -th pixel and n represents the region size in pixels.

Additionally, since during the BPT construction process regions of different sizes coexist, the region size information should be taken into account and will be included in the region model.

2. A similarity measure on the region model space to compare two neighboring regions $d(X, Y)$. Two types of measures are analyzed in this work, ones based on the statistical distribution (the Wishart distribution) and others based on the covariance matrix subspace geometry. The revised Wishart measure [KLA05] d_w is based on a statistical test assuming Wishart distributions and that one region statistics are known. However, since this measure is not symmetric, a modified symmetric version will be applied

$$d_{sw}(X, Y) = \frac{(tr(\mathbf{Z}_X^{-1} \mathbf{Z}_Y) + tr(\mathbf{Z}_Y^{-1} \mathbf{Z}_X))}{(n_x + n_y)} \quad (2)$$

where $tr(\cdot)$ represent the matrix trace, \mathbf{Z}_X and \mathbf{Z}_Y represent the estimated covariance matrices for regions X and Y , respectively, and n_x and n_y represent their number of pixels.

For comparison purposes a new version of the symmetric revised Wishart dissimilarity will be used, only taking into account the diagonal elements of the \mathbf{Z} matrix and assuming all off-diagonal values equal to zero

$$d_{dw}(X, Y) = \left(\sum_{i=1}^3 \left(\frac{Z_{Xii}^2 + Z_{Yii}^2}{Z_{Xii} Z_{Yii}} \right) \right) \cdot (n_x + n_y) \quad (3)$$

where Z_{Xij} and Z_{Yij} represent the (i,j) -th element of the estimated covariance matrices \mathbf{Z}_X and \mathbf{Z}_Y , respectively.

Another family of dissimilarities is proposed and analyzed on this paper based on the positive definite matrix cone geometry [Bar09]

$$d_{sg}(X, Y) = \left\| \log \left(\mathbf{Z}_X^{-1/2} \mathbf{Z}_Y \mathbf{Z}_X^{-1/2} \right) \right\|_F + \ln \left(\frac{2n_x n_y}{n_x + n_y} \right) \quad (4)$$

where $\|\cdot\|_F$ represents the Frobenius matrix norm, $\log(\cdot)$ represents the matrix logarithm and $\ln(\cdot)$ represents the natural logarithm.

As for the Wishart dissimilarities, a new version is defined employing only the information contained in the diagonal elements of the covariance matrix

$$d_{dg}(X, Y) = \sqrt{\sum_{i=1}^3 \ln^2 \left(\frac{Z_{Xii}}{Z_{Yii}} \right)} + \ln \left(\frac{2n_x n_y}{n_x + n_y} \right) \quad (5)$$

3. BPT PRUNING

The BPT is a hierarchical representation of the image structure at different details levels. Thus, it depends only on the image and consequently it is application independent. One possible approach to develop BPT-based applications is to select a set of meaningful regions within the tree. As mentioned in [SG00], an image segmentation can be obtained by tree pruning.

For the filtering application, the main target is to obtain the biggest possible homogeneous regions of the image. The BPT and its multi-scale nature can be exploited for this application. Then, an homogeneity-based tree pruning can be performed. A region homogeneity measure ϕ has to be defined to be able to define a pruning process. In [AGLMS10], is proposed the criterion based on the Frobenius matrix norm

$$\phi_R(X) = \frac{1}{n_x} \sum_{i=1}^{n_x} \frac{\|\mathbf{X}^i - \mathbf{Z}_X\|_F^2}{\|\mathbf{Z}_X\|_F^2} \quad (6)$$

where \mathbf{X}^i is the estimated covariance matrix for the i -th pixel within region X .

Note that this measure depends on all the pixel values within the X region and not only on its model, as the dissimilarity measure. Additionally, ϕ_R is independent of the region size, since it is an average over all the region pixels. This is an important property of the homogeneity measure in order to define the region homogeneity independently of its size. The measure (6) can be seen as the mean information loss when modeling all the pixels within a region with its estimated covariance matrix. Finally, to determine if a region is homogeneous or not, a maximum value δ_p for the homogeneity measure has to be defined, called *pruning threshold*. Then, the bigger regions X_i having $\phi_R(X_i) < \delta_p$ will be selected from the tree. In this paper δ_p will be expressed in dB scale, corresponding to $10 \cdot \log_{10}(\phi_R)$.

4. FILTERING RESULTS

The described homogeneity based BPT pruning for filtering has been tested with real and simulated PolSAR data. Fig. 1 shows one real image corresponding to PolSAR data that was acquired in a measurement campaign conducted by the DLR in 1999 with its experimental SAR system, E-SAR, over the Oberpfaffenhofen test-site, southern Germany. Data were collected at L-band, with a spatial resolution of $1.5m \times 1.5m$ in fully polarimetric mode.

On Fig. 2 different pruning results are shown over the same BPT constructed with the d_{sw} dissimilarity (2). Increasing the pruning threshold δ_p results in bigger regions of the tree pruned, as less homogeneous regions are accepted. Note that all of this regions are contained within

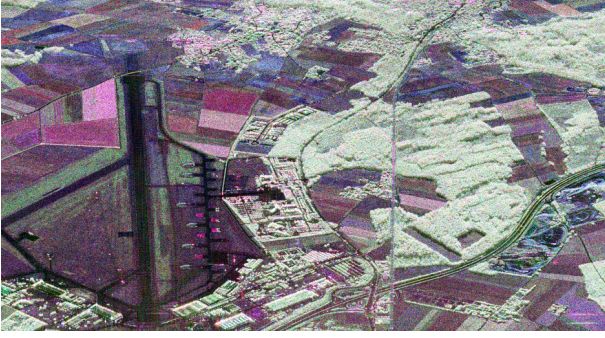


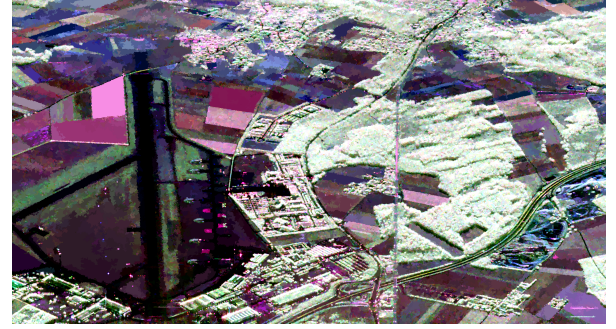
Figure 1: Pauli RGB original E-SAR image

the same tree and thus, they reflect the multi-scale nature of the BPT.

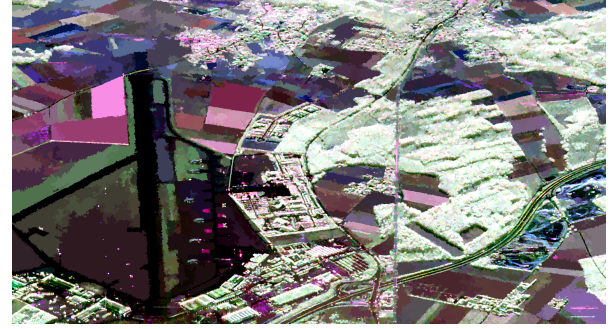
It is worth to notice that in the same image there are regions with very different sizes. Large homogeneous areas, as the agricultural fields in the left part of the image, appear as big regions whereas point scatters or details from the urban area in the center of the image are preserved as small regions. The value for each region is the estimated covariance matrix, as expressed in (1), over all the pixels within the region. This means that very strong filtering can be achieved while, at the same time, spatial resolution and small details of the image are preserved.

A 512x512 pixels cut of the original data, shown in Fig. 3a, is selected to see a more detailed view of the results. The 7x7 multilook is shown in Fig. 3b for comparison purposes. In Figs. 3c-3f different results are shown corresponding to the same tree pruning process over different BPTs constructed with the different similarity measures proposed. Compared with the 7x7 multilook, the BPT based filtering preserves much better original image spatial resolution and small details. Comparing the results obtained with different similarity measures there are very subtle differences. This fact gives an idea of robustness of the technique respect to the similarity measure employed for the BPT construction.

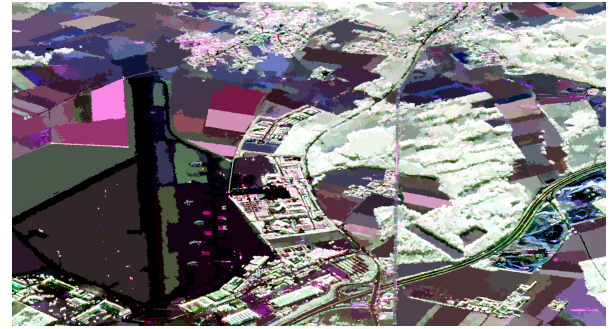
To analyze the capability of the BPT based filtering approach to retain the polarimetric information without distortion, the eigendecomposition parameters of the estimated covariance matrix, Entropy (E), Anisotropy (A) and the averaged alpha angle ($\bar{\alpha}$), are shown in Fig. 4. Different pruning thresholds are compared with the 7x7 multilook over the image cut presented in Fig. 3a. A qualitative analysis of these parameters shows that they obtain the same values. However, the BPT based filtering can take profit of the very large regions over homogeneous areas to enhance the covariance matrix estimation. This effect can be seen specially in the agricultural fields in the left part of the image. In the forest, in the right part of the image, the same effect can be found; increasing the pruning factor to $\delta_p = 0dB$ results in a better estimation of H and A, tending to 1 and 0 respectively, which fits with the theoretical response for random volume scattering. The capability to preserve small details can also be seen in urban areas, in the center of the image, specially



(a) $\delta_p = -2dB$



(b) $\delta_p = -1dB$



(c) $\delta_p = 0dB$

Figure 2: Pauli RGB processed images

in H and $\bar{\alpha}$ in comparison with the multilook, which has an important spatial resolution loss.

Additionally, a quantitative evaluation of the polarimetric information preservation has been made taking into account some homogeneous regions of the image presented in Fig. 5. Over these regions some parameters corresponding to covariance matrix elements and H/A/ $\bar{\alpha}$ decomposition have been estimated. The results for the original image, 7x7 multilook and BPT based filtering are shown in Table 1. The covariance matrix elements calculated for the original image and the filtered image are very similar for both filtering strategies. On some regions, the BPT pruning with $\delta_p = 0dB$ start to diverge from the original values due to inhomogeneous region mixture. The H/A/ $\bar{\alpha}$ parameters cannot be calculated over original data since it needs full-rank matrices and some filtering process is needed. The estimation of H and A parameters is biased [LMPC05] and, as stated

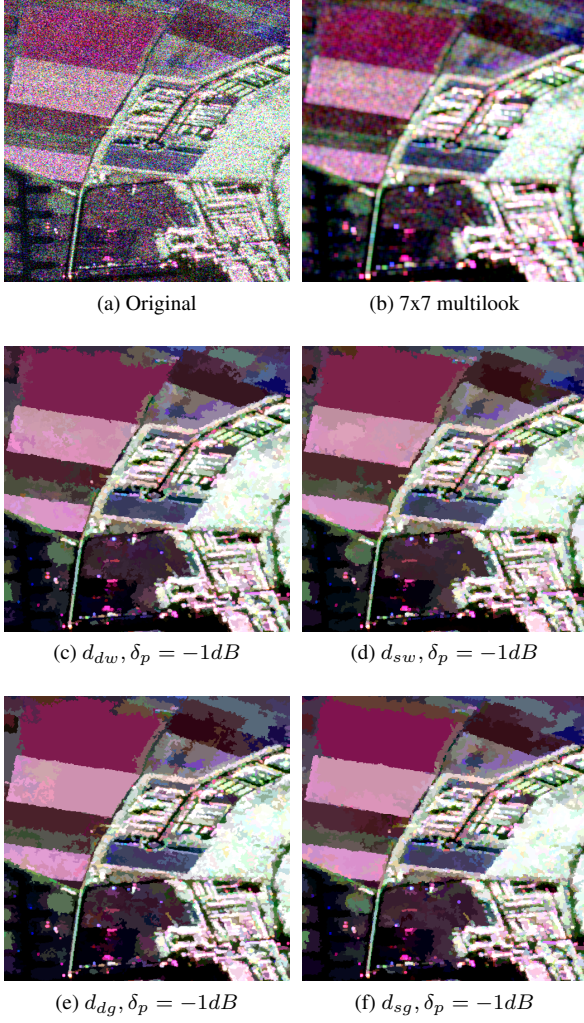


Figure 3: Detail Pauli RGB original and BPT processed images with $\delta_p = -1dB$ over different trees constructed employing various similarity criteria

before, the BPT based filtering can achieve a better estimation of the $H/A/\bar{\alpha}$ parameters due to the estimation of the covariance matrix over larger number of homogeneous samples. This explains the evolution observed for H and A , with are always underestimated and overestimated, respectively, when increasing δ_p .

To be able to make a quantitative evaluation of the BPT based filtering over the whole image a simulated data has been generated from a segmentation of a real image. A 512x512 pixels cut has been selected, Fig. 6a, containing mainly agricultural fields and some urban area, and it has been filtered using a BPT pruning with d_{sg} similarity measure and $\delta_p = -1dB$, Fig. 6b. This data has been used as a ground truth to generate simulated PolSAR images. A filtered image is employed in order to obtain a ground truth with realistic polarimetric and spatial information. As an example, one realization is shown in Fig. 6c and one BPT filtered image in Fig. 6d with d_{sg} similarity measure and $\delta_p = -5dB$.

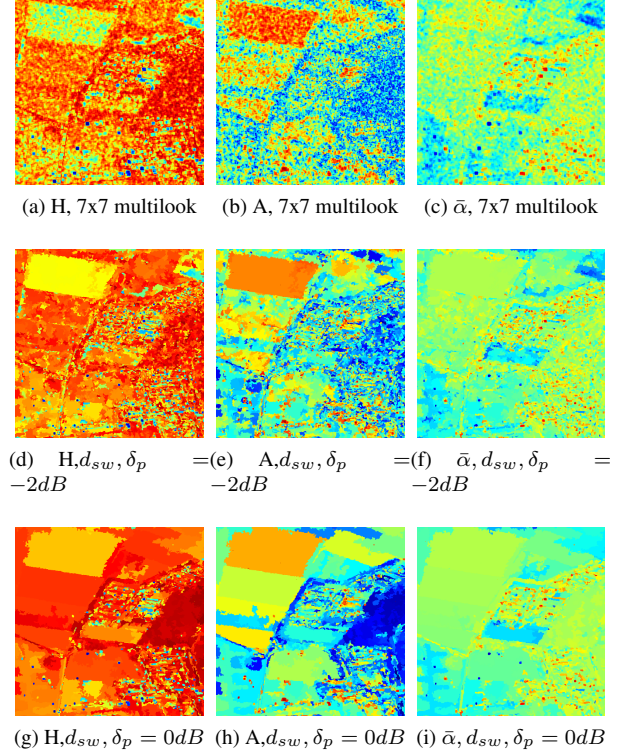


Figure 4: $H/A/\bar{\alpha}$ from processed images with multilook and BPT based pruning for different δ_p



Figure 5: Homogeneous zones selected over the image

Several different realizations are generated and filtered with different techniques. These results are compared with the ground truth, Fig. 6b, to asses numerically the goodness of the filtering technique. As an error measure, $E_R(X, Y)$ is defined between two images X and Y

$$E_R(X, Y) = \frac{1}{n_h \cdot n_w} \sum_{i=1}^{n_h} \sum_{j=1}^{n_w} \frac{\|\mathbf{X}^{ij} - \mathbf{Y}^{ij}\|_F}{\|\mathbf{Y}^{ij}\|_F} \quad (7)$$

where n_h and n_w are the image height and width in pixels, respectively, \mathbf{X}^{ij} represents the (i, j) th pixel value of image X and $\|\cdot\|_F$ denotes Frobenius matrix norm. Note that the relative error measure defined in (7) is based on the inverse signal to noise ratio (SNR^{-1}) averaged for all the pixels in the image.

Region	Filtering	C_{11}	C_{22}	C_{33}	$\Re(C_{13})$	$\Im(C_{13})$	H	A	$\bar{\alpha}$
Z1 5000 px	Original	28.27	16.06	18.34	5.242	5.504	-	-	-
	ML 7x7	28.21	15.97	18.36	5.321	5.465	0.8012	0.3543	48.29
	BPT -2dB	28.15	16.10	18.17	5.466	5.605	0.8271	0.2873	48.27
	BPT -1dB	28.20	15.20	18.08	5.558	5.612	0.8618	0.2036	47.91
	BPT 0dB	27.76	14.47	16.96	5.813	5.211	0.8694	0.1630	47.74
Z2 5950 px	Original	279.3	159.1	172.8	49.80	-14.37	-	-	-
	ML 7x7	280.8	159.3	172.9	49.18	-15.27	0.8598	0.2907	49.06
	BPT -2dB	278.1	158.4	171.5	48.05	-16.12	0.8475	0.2984	49.50
	BPT -1dB	280.4	157.7	172.4	50.24	-15.42	0.8925	0.2269	49.41
	BPT 0dB	292.2	160.8	177.0	50.74	-13.42	0.9305	0.1307	49.61
Z3 18000 px	Original	10.70	2.782	13.13	2.644	5.599	-	-	-
	ML 7x7	10.70	2.789	13.14	2.662	5.593	0.6781	0.4248	42.62
	BPT -2dB	10.33	2.713	12.94	2.498	5.255	0.7370	0.3755	43.32
	BPT -1dB	10.36	2.799	13.23	2.434	5.136	0.7445	0.3881	43.60
	BPT 0dB	11.76	3.405	13.59	2.556	5.351	0.7852	0.3471	44.34

Table 1: Mean estimated values over homogeneous areas for different filtering strategies

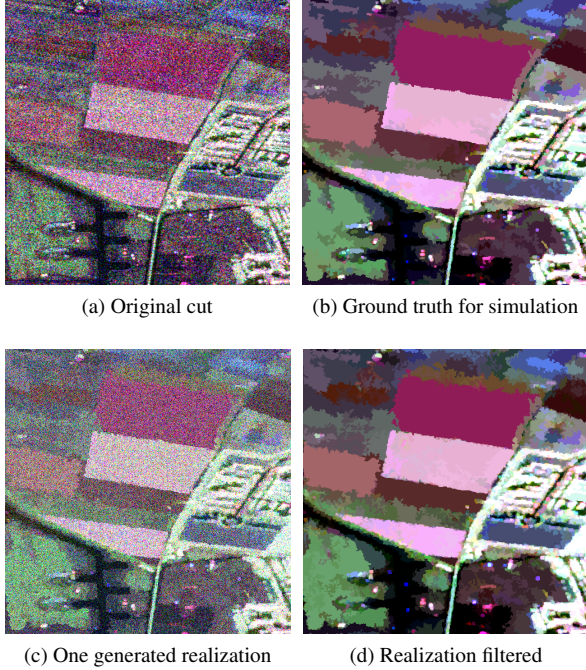


Figure 6: Simulated data generation from a real image segmentation

Fig. 7 shows the evolution of the relative error E_R defined in (7) when changing the pruning threshold δ_p for the defined similarity measures in Section 2. Note that the error axis is expressed in logarithmic scale (dB). To make a clearer plots, results over 25 different realization of the ground truth have been averaged. As it can be seen, the behavior when changing the pruning factor is the same for all the BPTs constructed with different criteria. There is always a clear minimum located at about -5dB. According to the relative error E_R criterion, employing the diagonal similarity measures for BPT construction seems to achieve better results than full-matrix ones. However,

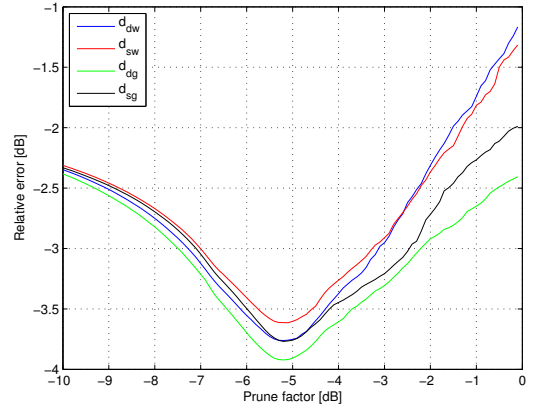


Figure 7: Relative error E_R versus pruning factor δ_p plot over simulated images

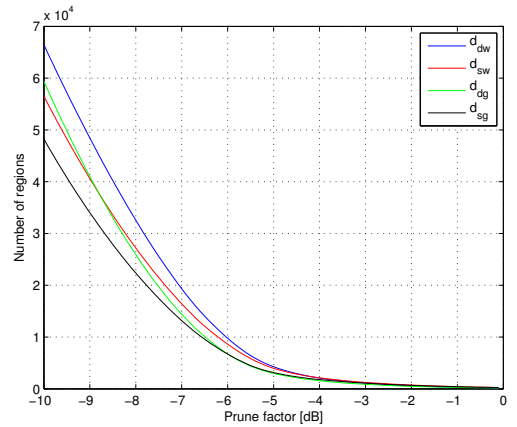


Figure 8: Number of regions versus pruning factor δ_p plot over simulated images

the E_R measure is more sensitive to power, corresponding to the diagonal elements of the covariance matrix,

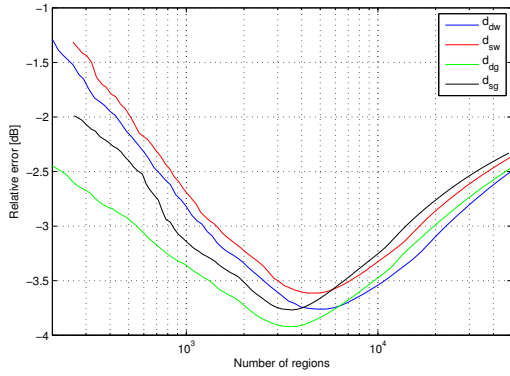


Figure 9: Relative error E_R versus number of regions plot over simulated images

than to the correlation information. In the lack of a clear measure to correctly quantify the polarimetric information loss, an alternative evaluation is made by means of analysis of the number of regions attained by different BPT pruning in Fig. 8. Note that the number of regions pruned is automatically found when fixing the maximum accepted homogeneity per region δ_p . This plot shows that for a specific value of δ_p , the number of regions attained by full-matrix similarity measures is always lower than for the diagonal ones. This means that full-matrix similarity measures produce trees having bigger regions with the same level of homogeneity and, thus, they can achieve better adaptation to the spatial information. Additionally, it reflects that similarity measures based on the positive definite covariance matrix cone geometry leads to better adaptation to this spatial information than the ones based on the Wishart distribution statistical test.

Moreover, Fig. 9 shows the relative error E_R versus the number of regions pruned. Similarity measures based on the positive definite matrix cone geometry attain better results in terms of relative error and also they achieve the best results with a lower number of regions than the Wishart based ones. As a reference, the ground truth image, Fig. 6b, has 1939 regions, whereas the minimum error is attained at 3000-4000 regions for d_{dg} and d_{sg} and over 5000 for d_{dw} and d_{sw} measures. This difference reflects the accuracy of the different segmentations obtained by means of BPT pruning and, consequently, the quality attainable for the filtering application.

Analyzing the results with real and simulated data an important point arises. Similar results are obtained by means of BPT based filtering in Fig. 6b and Fig. 6d in real and simulated images. However, the pruning threshold in both cases differs significantly: -1dB and -5dB, respectively. In the view of the authors, this fact can be related to additional region features in the real data not taken into account inside the model, which can be considered as the region texture. The homogeneity threshold has to be increased to absorb these modeling errors with real data. For the simulated data, since this texture is not reproduced, it is not necessary to increase δ_p and the same

results are obtained with lower homogeneity thresholds.

5. SEGMENTATION RESULTS

In Section 4 the BPT has been analyzed to develop a filtering application. However, the BPT is an application independent image representation that can be useful for many other applications. As an example, in this section some results will be shown that employ the BPT for a segmentation application, concretely to coastline segmentation. For filtering purposes, the pruned nodes are usually homogeneous regions that are relatively close to the tree leaves. For this application, bigger regions are interesting, strongly non-homogeneous, closer to the tree root.

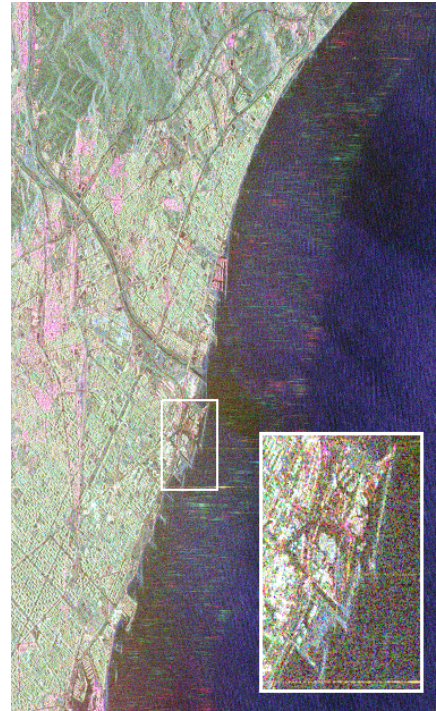


Figure 10: Pauli RGB for the original image of Barcelona

Fig. 10 shows the original image corresponding to 1500×2500 -pixel cut of a C-band Pauli RADARSAT-2 image of Barcelona, Spain, that was acquired in November, 18th 2008, in fine quad polarization mode with nominal resolution of $5.2m \times 7.6m$. The figure also shows a detailed area corresponding to the Forum harbor of Barcelona. Fig. 11 shows the resulting coastline segmentation result. Two regions can be clearly seen, corresponding to the land and the sea on the original image. In this case the pruning process is based on selecting the two bigger regions of the tree, corresponding to the two sons of the root node. Fig. 11 represents the entropy H of the two regions. The d_{sw} criteria has been used for BPT construction, defined in (2). As can be seen, specially in the zoom over the Forum harbor, the segmentation preserves the spatial resolution of the original image and small details and thin structures like breakwaters are preserved.

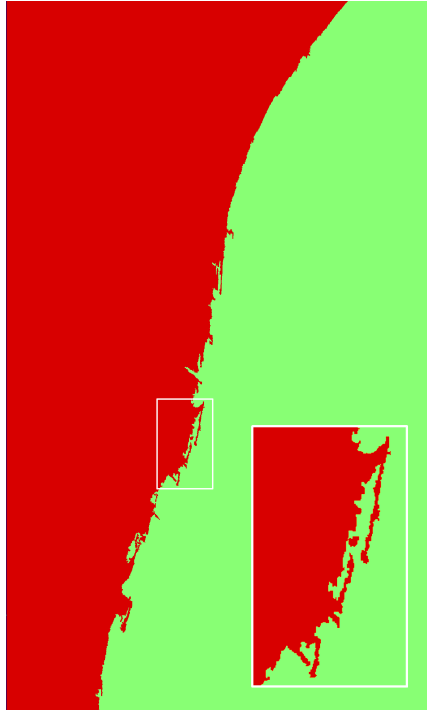


Figure 11: Coastline segmentation, where colors represent the region entropy H

6. CONCLUSIONS

In this work, a region-based and multi-scale image representation has been employed for PolSAR data representation [AGLMS10]. This BPT representation contains information about the image structure and is application independent. It has proved to be able to extract spatial information of the image at different detail levels, ranging from small details close to the tree leaves to big regions close to the root, as the land and the sea on the segmentation example.

An iterative algorithm is employed to construct a BPT from a PolSAR image, based on a region model and a similarity measure. The region model is based on the polarimetric information contained in the covariance matrix and several similarity criteria are presented. Analyzing the results obtained for the filtering application, it seems that the proposed family of measures based on the positive definite matrix cone geometry perform better for BPT construction since a better adaptation to the spatial information is achieved.

In addition, a BPT based processing approach is analyzed, based on an application dependent tree pruning, which produces a segmentation of the image. The speckle filtering application has been studied in detail, by defining a BPT pruning based on the region homogeneity. It has proved to attain good results with real and simulated data, being able to obtain at the same time large regions over homogeneous areas while preserving spatial resolution and small details. Moreover, this filtering tech-

nique is able to adapt to the full polarimetric information without introducing any kind of bias or distortion. Additionally, the segmentation application itself has been presented with a coastline segmentation example. On this example a simpler pruning process is employed: select the two bigger regions of the BPT, corresponding to the soon nodes of the tree root. Furthermore, the BPT representation contains a lot of information about the image that can be useful for many other applications.

ACKNOWLEDGMENT

The authors would like to thank to DLR and to MDA for providing the ESAR and the RADARSAT-2 datasets, respectively.

REFERENCES

- [AGLMS10] Alberto Alonso-Gonzalez, Carlos Lopez-Martinez, and Philippe Salembier. Filtering and segmentation of polarimetric sar images with binary partition trees. In *Proc. IEEE Int. Geoscience and Remote Sensing Symp. (IGARSS)*, pages 4043–4046, 2010.
- [Bar09] Frederic Barbaresco. Interactions between symmetric cone and information geometries: Bruhat-tits and siegel spaces models for high resolution autoregressive doppler imagery. In Frank Nielsen, editor, *Emerging Trends in Visual Computing*, volume 5416 of *Lecture Notes in Computer Science*, pages 124–163. Springer Berlin / Heidelberg, 2009.
- [KLA05] P. R. Kersten, Jong-Sen Lee, and T. L. Ainsworth. Unsupervised classification of polarimetric synthetic aperture radar images using fuzzy clustering and em clustering. *IEEE TGRS*, 43(3):519–527, 2005.
- [LGdG99] Jong-Sen Lee, M. R. Grunes, and G. de Grandi. Polarimetric sar speckle filtering and its implication for classification. *IEEE TGRS*, 37(5):2363–2373, 1999.
- [LMPC05] C. Lopez-Martinez, E. Pottier, and S. R. Cloude. Statistical assessment of eigenvector-based target decomposition theorems in radar polarimetry. 43(9):2058–2074, 2005.
- [SG00] P. Salembier and L. Garrido. Binary partition tree as an efficient representation for image processing, segmentation, and information retrieval. *IEEE TIP*, 9(4):561–576, 2000.
- [VTLB06] G. Vasile, E. Trounev, Jong-Sen Lee, and V. Buzuloiu. Intensity-driven adaptive-neighborhood technique for polarimetric and interferometric sar parameters estimation. *IEEE TGRS*, 44(6):1609–1621, 2006.